European Organization for Nuclear Research
CERN AB Departement

CERN-AB-Note-2008-016

Design of a Spin-Flip Cavity for the Measurement of the Antihydrogen Hyperfine Structure

T. Kroyer

Abstract

In the framework of the ASACUSA collaboration at the CERN Antiproton Decelerator an experiment for precisely testing the CPT invariance of the hydrogen hyperfine structure is currently being designed. An integral part of the set-up is the 1.42 GHz spin-flipping cavity, which should good have a good field homogeneity over the large aperture of the antihydrogen beam. After the evaluation of various approaches a structure based on a resonant stripline is proposed as a concrete cavity design. For this structure the field homogeneity, undesired modes, coupling and power issues are discussed in detail.

Geneva, Switzerland
April 2008

1 Introduction

The ASACUSA collaboration at the CERN Antiproton Decelerator (AD) is planning to measure the charge-parity-time reversal (CPT) invariance of the hydrogen hyperfine structure [1]. The hyperfine splitting of the 1s ground state due to the coupling of the proton and electron magnetic moments in hydrogen corresponds to a transition frequency of $f = 1.42$ GHz. The experimental layout for measuring this frequency for antihydrogen ($\overline{\mathrm{H}}$) is illustrated in Fig. 1. $\overline{\mathrm{H}}$ atoms are formed in the recombination trap on the left. In the nonlinear magnetic field of the first sextupole two $\overline{\mathrm{H}}$ states are selected according to their magnetic moment (solid trajectory) while atoms in the other two states are lost (dashed trajectories). If there is no field in the microwave cavity the atoms in the selected states will continue drifting along the solid line through the second (analyzing) sextupole and be counted at the detector at the end of the line.

In order to determine the hyperfine frequency, an RF magnetic field is established in the cavity. A frequency scan in the region of the expected transition is done and the $\overline{\mathrm{H}}$ counts plotted as a function of frequency. When the hyperfine transition is hit, the atoms' spins flip and the atoms follow the dashed trajectory in the second sextupole. The hyperfine transition frequency is found by the corresponding dip in the number of $\overline{\mathrm{H}}$ arriving at the detector.

For the ASACUSA experiment the parameters relevant to cavity are as follows [2]:

- Magnetic RF field of 10^{-6} T averaged along the beam trajectory.
- The length of the cavity should be within 100 to 400 mm. Along the trajectory of the beam the H field may vary, e.g. sinusoidally, however the field pattern must be exactly known in order to predict to behaviour of the $\overline{\mathrm{H}}$ atoms.
- Beam cross-section circular with 100 mm diameter.
- The magnetic field should be homogeneous transversely over the beam aperture to within ±10%.
- The transverse size of the cavity is not very critical; the tank diameter should not exceed ≈ 400 mm.

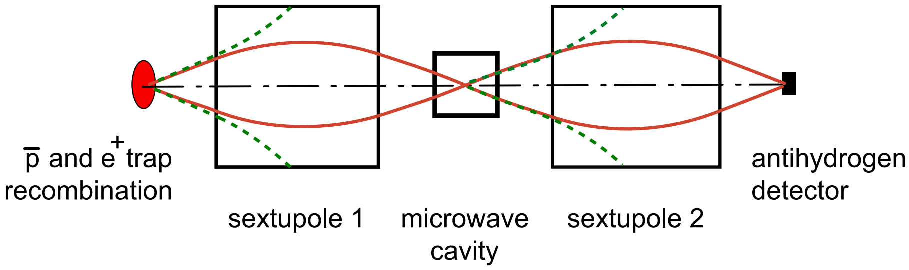

Figure 1: Schematic drawing of the hyperfine splitting measurement. One state of the antihydrogen atoms coming from the recombination in the trap on the left is selected by the first sextupole, cross the second sextupole and reach the detector. When the spin flipping cavity is tuned to the hyperfine frequency the $\overline{\mathrm{H}}$ spin states are flipped; the atoms are then lost in the second sextupole. Figure courtesy of B. Juhasz.

- The H field should have no components in the direction of the beam.
- A bandwidth of 4 MHz centered at the nominal transition frequency of 1.4204 GHz should be accessible, which implies a maximum quality factor of $Q = 355$.
- The RF field should preferably be a standing wave and not a traveling wave in the beam direction to avoid Doppler shifts.
- Furthermore a small static H field at an angle of about 45° with respect to the RF H field is needed, however since the static field is easier to set up no particular attention needs to be paid here.

Similar experiments have been done for ordinary hydrogen and hydrogen masers are operated using the same principles. With $\overline{\mathrm{H}}$ atoms the difficulty consists in creating a thin pencil beam, since antihydrogen production is notoriously difficult and expensive. In order to capture a maximum number of $\overline{\mathrm{H}}$ atoms the acceptance of the experiment was maximized, which makes the design of a homogeneous RF magnetic field over the entire beam cross-section more complicated.

In the next section several cavity designs are presented and evaluated and the most promising structure identified, which is then discussed in detail. For the numerical simulations the package CST Microwave Studio was used [3].

2 Design ideas

For the present application ideally we should provide a perfectly homogeneous purely transverse RF magnetic field, such as a small part of a homogeneous plane wave (HPW). The structures presented in the next sections try to approach the properties of a HPW in different ways. Most solutions can be implemented as traveling wave structures as well as with standing waves. These two options are compared before discussing concrete examples.

2.1 Traveling wave versus standing wave structures

For physics reasons there is a slight preference for standing wave structures, however traveling wave solutions should also be considered. Since the present application does not require a large bandwidth, Q factors of the order of 100 can be used, which reduces the required RF power. In addition to that the beam aperture is comparable to the total structure length (100 mm compared to 100 to 400 mm). Therefore fringe field effects are very important in traveling wave structures. For these reasons all the designs presented below are standing wave-type structures.

2.2 Ordinary cavity

It is possible to get a field pattern close to the desired one by using a simple TM_{010} cavity (Fig. 2). In the center of the $\overline{\mathrm{H}}$ beam (z axis) the H field is indeed purely transverse. Longitudinally, the H field has one half period, which would be acceptable. However, moving off-center it decreases and undesired longitudinal field components (in z direction) appear. It is possible to reduce the H field in the z direction by increasing the cavity size, but for too large dimensions more and more higher order modes come into play and the design gets impractical.

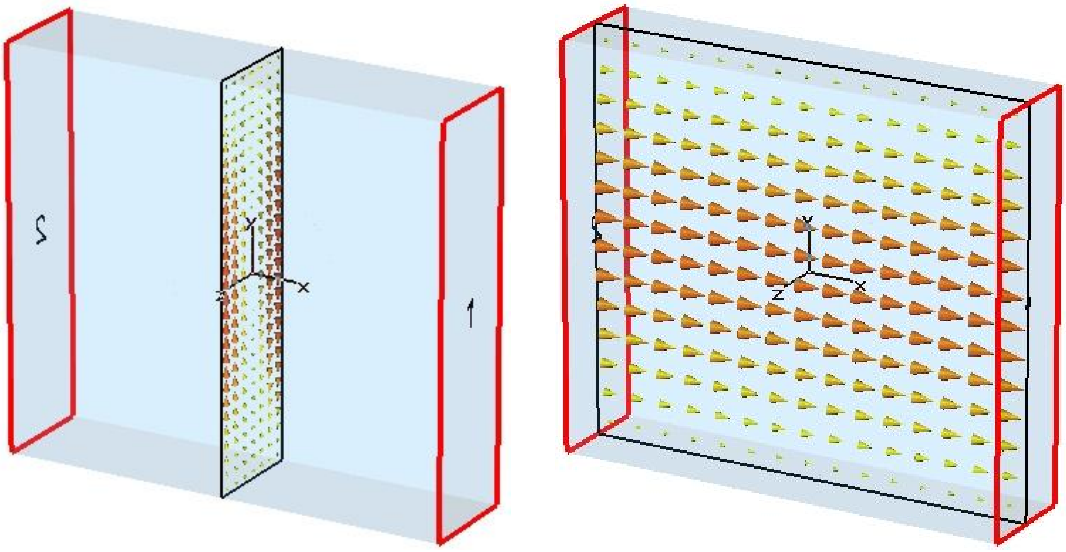

(a) Magnetic field. (b) Electric field.

Figure 2: A thin TM_{010} cavity. The $\overline{\mathrm{H}}$ bar atoms travel along the z axis. On the beam axis the H field is purely transverse, but off-axis there are longitudinal components, which is not desired.

2.3 Resonant stripline

In order to avoid longitudinal H field components the H field loops must be chosen to close on the side of the structure. This is possible e.g. for a stripline which is excited in the odd mode, i.e. the currents run in opposite directions. For a sufficiently wide stripline the magnetic field becomes very homogeneous in the center of the line. If such a structure is mounted in a vacuum tank fringe fields appear at the beginning and end of the structure. In order to minimize them the striplines can be shorted to the tank at both ends, which leads to a resonant double stripline (Fig. 3). The beam goes along the z axis; its aperture is marked with a light blue circle at the front and back of the structure. A transverse field homogeneity of $\pm 3\%$ was obtained for the present example, which is amply sufficient.

Along the beam axis the H field varies sinusoidally with maxima at the beginning and end of the structure. Possible structure lengths are integer multiples of $\lambda/2$, i.e. 105.5 mm, 211 mm etc (Fig. 4).

Since the double stripline inside a tank represents a 3-conductor system, it can support two degenerate transverse electromagnetic (TEM) modes as depicted in Fig. 5. This situation is not changed fundamentally by shorting the ends of the striplines. Although the two modes are detuned due to end effects, the resonance frequencies stay close together. In order to use only the desired odd mode the even mode has be to suppressed by appropriate excitation or the structure has to be modified such as to selectively detune the modes. However, even if the even mode is weakly excited this should not have disastrous consequences since its field components in the beam aperture are small.

An option for making the structure easier to use and to exclude the undesired even mode is shown in Fig. 6. Here the second stripline is removed, which leaves us with a

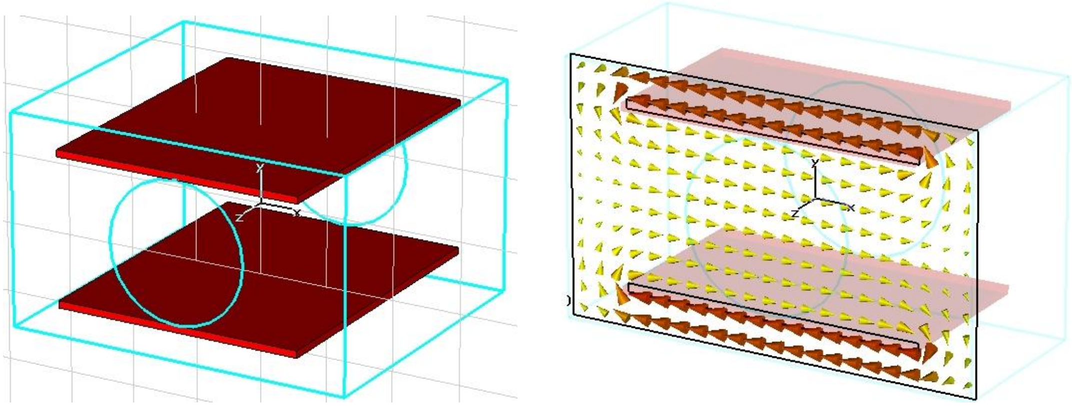

(a) Structure of the resonant stripline. The striplines (red) are shorted to the tank on the front and back.

(b) Magnetic field. The field lines close behind the striplines outside the beam aperture.

Figure 3: The resonant stripline offers a good transverse field homogeneity. The beam drifts along the z axis, its aperture is sketched with the circles in the front and back of the structure.

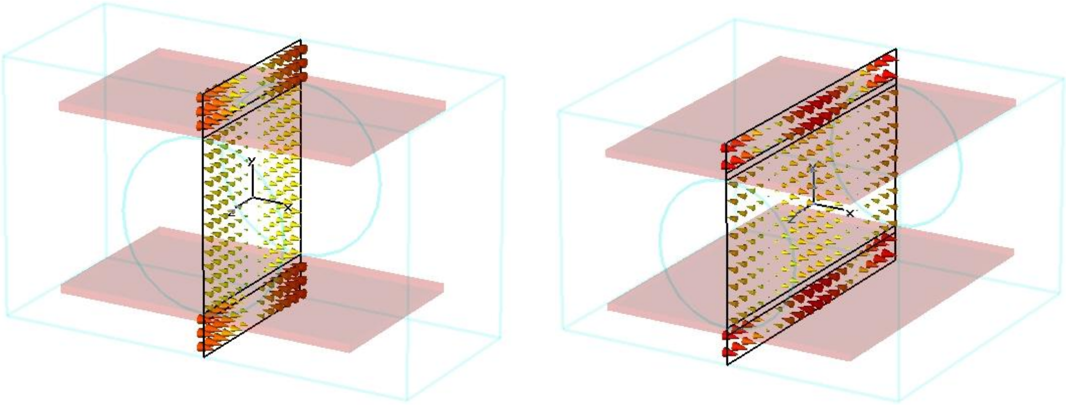

(a) A $\lambda/2$ structure.

(b) A λ structure.

Figure 4: The magnetic field in the resonant stripline along the beam axis.

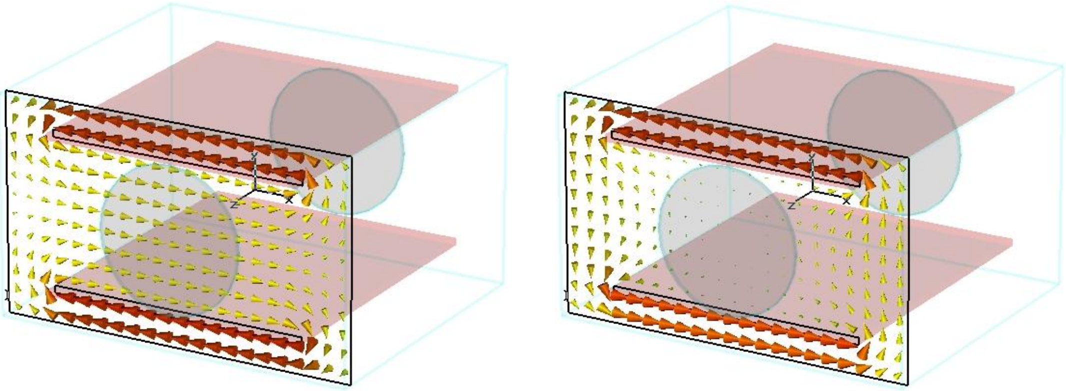

(a) The desired odd mode.

(b) The undesired even mode.

Figure 5: The two degenerate modes on a double stripline.

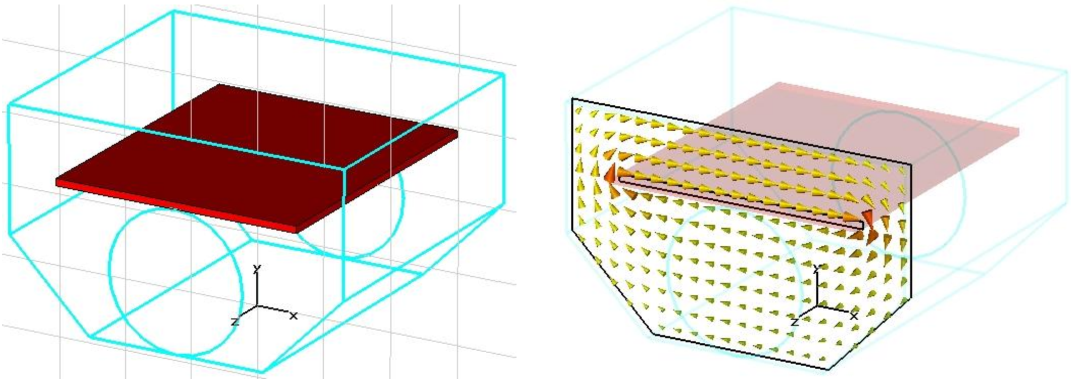

(a) Structure.

(b) Magnetic field.

Figure 6: The single resonant stripline has less good transverse field homogeneity, but only a single mode can exist at the resonant frequency. It is simply a shorted coaxial line. The beam drifts along the z axis, its aperture is sketched with the circles in front and back of the structure.

simple coaxial resonator. Unfortunately the field homogeneity is substantially affected, it is only within ±15%, and is out of specification.
So far only ideal metallic cavities were considered, but of course the beam has to enter the cavity at some location. This is usually done by adding a metallic mesh with high (optical) transparency. Thus most of the $\overline{\mathrm{H}}$ atoms can pass while the RF sees an almost perfect cavity.

2.4 Magnetic wall

An elegant option was suggested by F. Caspers: A perfectly transverse H field can be obtained in a cavity such as in Fig. 2 or in a waveguide by using “magnetic walls”, i.e. walls where the magnetic field components are exclusively normal. This is obvious and can be easily checked by simulation by choosing the appropriate boundaries (Fig. 7). However, unfortunately the practical implementation appears to be less obvious. Such

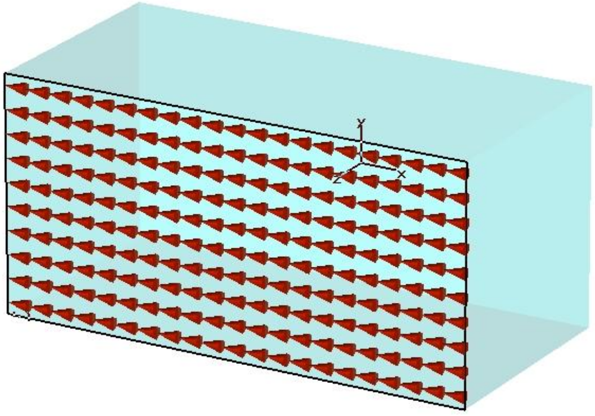

Figure 7: H field in a structure with ideal magnetic walls on the right and left side.

high-impedance surfaces have been implemented as microstructures in printed circuit technology for antenna design, see e.g. [4] and references therein. These structures only work in a certain frequency band, which would be fine for the present application. However, it is hard to predict how well the suppression of the longitudinal field will work. Including printed circuits in a ultra-high vacuum (UHV) environment is difficult and the length of the resonator would depend on the exact properties of the magnetic wall, which could make several iterations in the design, manufacturing and testing process necessary.

2.5 The most promising candidate

The choice of using a resonant structure was taken due to the fringe field related problems common to all traveling wave structures considered. Among the cavities, the TM_{010} mode was excluded due to the unavoidable longitudinal field components. Other cavity modes don't meet the field homogeneity requirements. Even though very attractive in theory, structures with magnetic walls appears to be exceedingly difficult to implement. This leaves the resonant stripline as the most promising candidate, as it offers the required field homogeneity and can be readily implemented in practice. Since the desired field homogeneity is hard to achieve using a simple coaxial structure the double stripline was chosen. The additional effort related to mode excitation appears manageable. In the next section a concrete design is presented.

3 Concrete design: The resonant stripline

As the most promising candidate for the $\overline{\mathrm{H}}$ spin-flip cavity the resonant double stripline was chosen (Fig. 8). Both striplines are shorted to the metallic tank on both ends. The beam goes along the z axis, its cross-section is marked with the light blue circles. For physics reasons the $\lambda/2$ length version was selected. This is motivated by simulations which predict that due to the standing wave in the cavity more than a single dip in the antihydrogen count will be found for a frequency scan [2]. The number of dips is equal to the number of magnetic field maxima along the beam axis. A length of $\lambda/2$ gives rise to two dips, which is sufficiently easy to interpret. A standard round tank

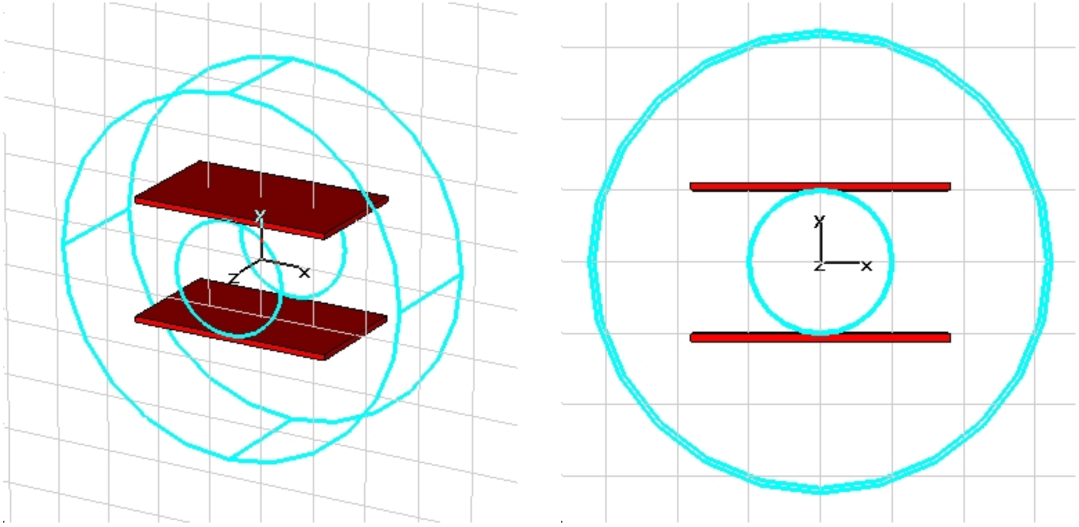

(a) Perspective view. (b) Front view.

Figure 8: The structure of the resonant stripline. The $\overline{\mathrm{H}}$ beam drifts along the z axis, the light blue circles represent the beam cross-section. The striplines (red) are shorted to the tank at both ends.

with 320 mm diameter was selected. The width of the striplines was adjusted such as to get a good transverse field homogeneity. The stripline thickness is not very critical. Table 1 summarizes the main parameters.

From the required 4 MHz operational bandwidth it follows that the quality factor $Q \leq 355$. However, since the required input power is not excessive the Q factor should better be lowered by overcritical coupling to $Q \approx 100$. This provides for a robust design and eases the mechanical tolerances. The dominant factor determining the resonance frequency is the length of the inner section consisting of the striplines and the end caps, as the field is maximal there. In order to stay well within the 1% bandwidth the mechanical tolerances on the length should be well below 0.5%. In practice mechanical tolerances of 0.1% should be reasonable to obtain, since this corresponds to 0.1 mm in the stripline length.

3.1 Field homogeneity

The H field pattern is depicted in Fig. 9. This mode is the odd mode of the stripline, i.e. the voltages and currents on the top and bottom plate are out of phase. A transverse field homogeneity of ±2% was achieved. On the top and bottom of the beam aperture the field is slightly higher and towards to sides it is lower than in the center. The adjacent beam pipe has a diameter of 100 mm, corresponding to waveguide cut-off at 1760 MHz. Therefore only evanescent fields are possible in the beam pipe. In order to minimize these fields, the ends of the beam pipe have to be shielded with a conductive mesh. As long as this mesh is sufficiently fine the field pattern should not be influenced much, but the losses will reduce the quality factor of the cavity.

Parameter	Unit	Value
Resonant frequency	MHz	1420.4
3 dB bandwidth	MHz	≈14
Loaded Q factor	1	≈100
peak magnetic field	T	10^{-6}
input power ($Q = 100$, on resonance)	mW	310
structure length	mm	105.5
tank diameter	mm	320
electrode width	mm	180
electrode thickness	mm	5
coupling pin length	mm	≈20
coupling pin diameter	mm	5
wing length	mm	53
wing width	mm	36
wing thickness	mm	2

Table 1: Parameters for the resonant stripline, according to the illustrations in Figs. 8, 11(a) and 12.

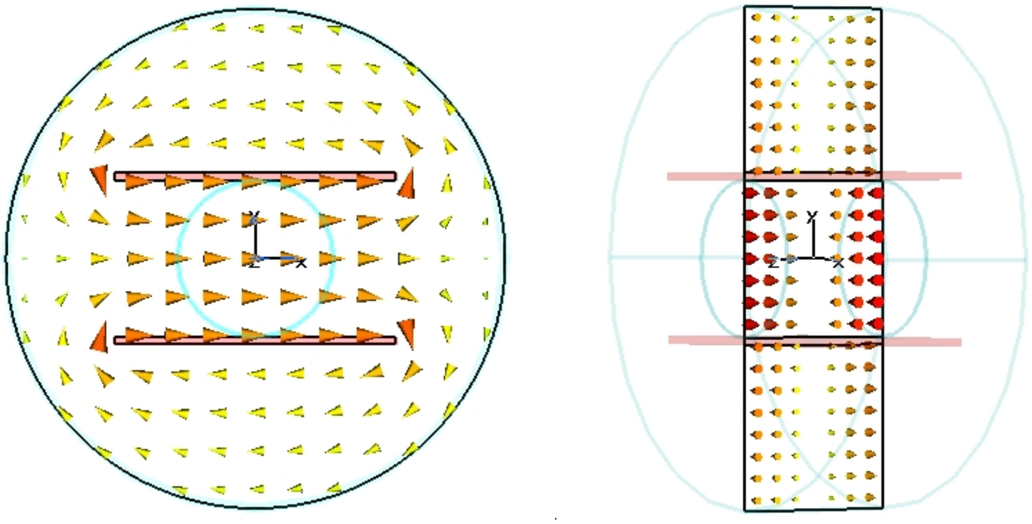

(a) Transverse cut.

(b) Longitudinal cut.

Figure 9: The H field in the resonant stripline. The strip width was adjusted for good transverse field homogeneity (within ±2%). The length of the structure is $\lambda/2$.

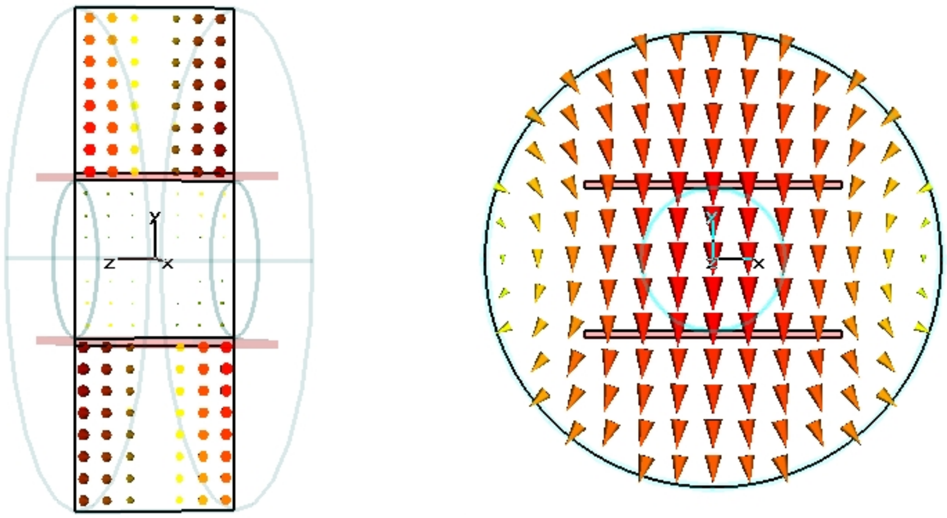

(a) The even TEM mode has about the same resonance frequency as the desired odd mode (H field plotted).

(b) The closest higher order mode with the same symmetry as the desired mode is similar to the TE_{101} mode in the empty cavity (E field plotted).

Figure 10: The two principal undesired modes on the resonant stripline.

3.2 Undesired modes

Fig. 10 shows the two principal undesired modes in the structure. On the left is the even mode of the stripline structure, which has about the same resonant frequency as the desired odd mode. It can be avoided by mode-selective excitation or by detuning it, as will be shown below. In the right picture is a mode similar to the TE_{101} in the empty cavity with resonant frequency at 1520 MHz. Since this mode's field pattern is very similar to the desired mode, it is difficult to suppress, so we have to make sure it is sufficiently far away in frequency, which is the case for the current structure.

Fig. 11(a) shows that a small modification of the layout can selectively detune the undesired even mode, as suggested by W. Pirkl. The odd mode H field is purely transverse in the horizontal center plane (Fig. 5(a)), while the even mode H field is vertical (Fig. 5(b)). A horizontal metallic plane inserted at this position therefore exclusively affects the undesired mode. The inserted piece must be inhomogeneous longitudinally, since otherwise we just get another TEM structure with a different outer conductor cross-section but degenerate modes. Among various different insertions, wings in the center of the cavity as depicted in Fig. 11(a) gave the largest detuning effect. The undesired mode splits up in two modes with resonance frequencies around 1285 MHz. The desired odd mode is not affected (Fig. 11(b), $f = 1420$ MHz), higher order modes exist at 1511, 1520, ... MHz. It turned out that the chosen tank diameter of 320 mm is close to the maximum possible value, since already for slightly larger diameters (360 mm) many modes exist in the vicinity of the 1420 MHz operational frequency.

3.3 Coupling

In order to selectively excite the odd mode, two coupling elements driven with opposite phase are necessary. Capacitive pins were preferred over inductive loops, since pins are

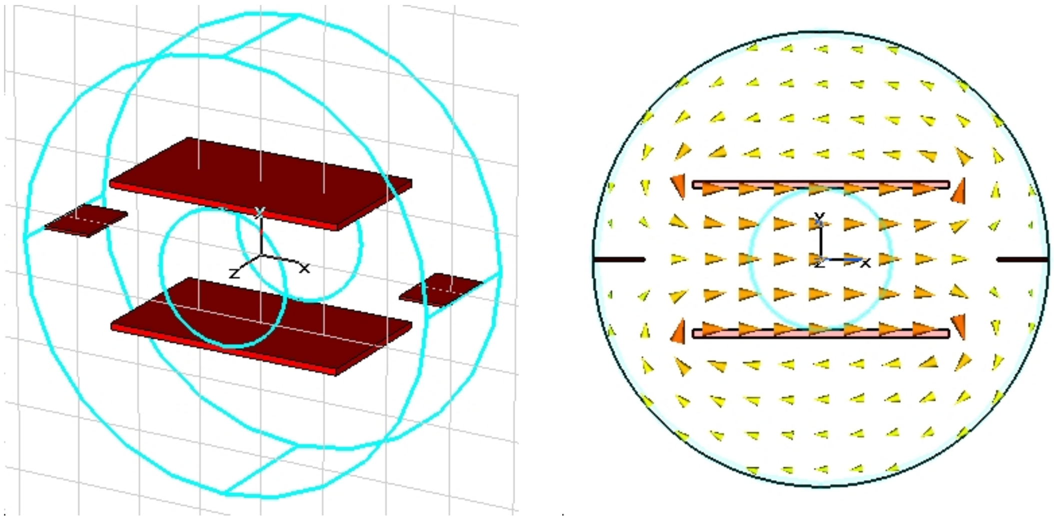

(a) The resonant stripline with wings.

(b) The field pattern of the desired odd mode is hardly affected by the insertion of the wing.

Figure 11: By adding a horizontal wings in the middle of the cavity the degeneracy of the even and odd modes can be broken.

very simple elements and strong overcoupling can still be obtained for large enough pin lengths. The pins have to be positioned at the top and bottom of the tank (Fig. 12). They can be mounted on standard 50 Ω Conflat (DN 16 CF) UHV feedthroughs. In Fig. 12(b) the part of the pin protruding into the tank has a diameter of 7 mm, the same as in the 50 Ω section inside the feedthrough. However, the pin diameter is not a critical parameter. A thinner pin has to be prolonged by about the difference in radius to compensate for the smaller end effects.

Strong overcoupling is necessary to obtain the loaded Q of $Q_L = 100$. The coupling strength can be adjusted by changing the length of the coupling pins. For 7 mm diameter critical coupling is expected for 10 mm pin length; 20 mm pins should give strong overcoupling.

External components

Fig. 13 shows the components needed to generate the signals for the two feedthroughs. The signal from the RF generator is split in a 3 dB hybrid to get two feed signals with opposite phases. The sum output of the hybrid has to be terminated with a matched load in order to damp undesired modes in the cavity. Between the generator and the hybrid a variable matching network, e.g. a triple stub tuner can be inserted for flexible adjustment of the match and the coupling strength. In practice, the pin length can be varied in a few iterations to get the coupling parameter into the right range, while the fine adjustment is done with the triple stub tuner.

An alternative way could be to rely exclusively on the frequency separation of the undesired modes and feed one single pin only. Changing the coupling parameter by varying the pin length would then be easier.

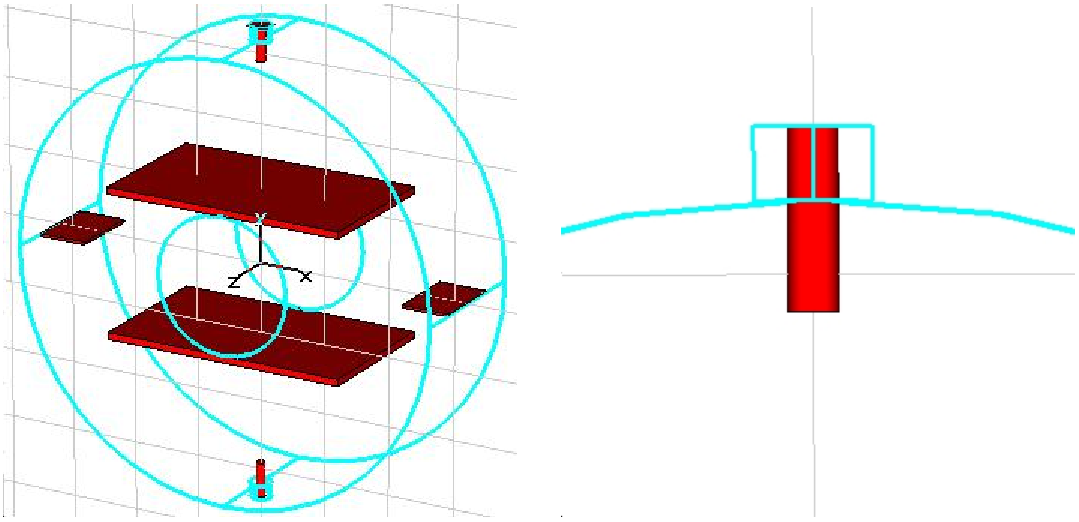

(a) Perspective view of the full cavity with coupling pins and wings.

(b) Detail: the coupling pin.

Figure 12: Coupling of the cavity to the external world can be done using a capacitive pin on the top and bottom.

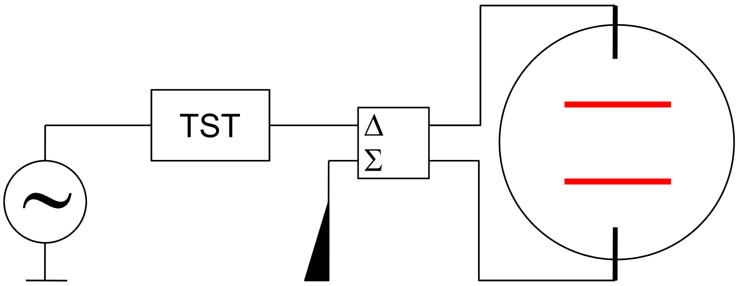

Figure 13: Schematic view of the external circuitry connected to cavity. The top and bottom feedthrough are fed in phase opposition via a hybrid. The common mode signal from undesired modes reaching the hybrid is dissipated in an RF load. A triple stub tuner (TST) can be used for matching and adjustment of the coupling strength.

Cavity \ mesh	no mesh	copper	stainless steel
copper	15100	5440	1170
stainless steel	2350	1960	845

Table 2: Q values for the resonant stripline with and without meshes at the end of the beam pipe.

3.4 Q factor

The unloaded Q factor Q_0 of the cavity was evaluated in the numerical simulation for cavities made of copper ($\sigma = 58$ MS/m) and stainless steel ($\sigma = 1.4$ MS/m). The effect of the meshes at the beam aperture was estimated under the assumption that the cavity field is only little perturbed by the presence of the mesh. For a typical 95% transparency only 5% of the surface is available for the wall currents and the current density increases by a factor 20. The total losses are proportional to the square of the current density times the available surface; they also increase by a factor 20. This can be modeled by a 400 times higher resistivity. Of course this estimate is very pessimistic, since it is assumed that current flows only on a surface given by the projection of the mesh along the beam axis; for a thick mesh the available surface can much larger. The Q_0 values for cavities without and with mesh are given in the Table 2. Quality factors in the range of 1000 should be obtainable with the cavity and the meshes made of stainless steel. The losses on the tank and stripline are much smaller than on grids made of the same material.

3.5 Required power

The stored energy in the cavity W is proportional to the square of the peak magnetic field at the ends of the structure

$$W \propto \hat{B}. \tag{1}$$

From the numerical simulation it is known that in order to get a *peak* magnetic field on the beam axis $\hat{B} = 10^{-6}$ T we need $W = 3.44$ nJ. The dissipated power depends on W and the quality factor Q as

$$P = \frac{\omega W}{Q}. \tag{2}$$

Therefore, with $Q_L = 100$ the dissipated power on resonance is $P = 0.31$ W. For operation within the 3 dB bandwidth the required input power increases by a factor two. Including losses in the feed lines and hybrid plus an engineering margin raises the required power rating for the generator or amplifier by another factor of two to about 1.2 W.

Due to low field in the cavity and the large stripline spacing multipactor is not expected.

3.6 Tuning

Since the electric and magnetic fields in the resonant stripline are concentrated between the two plates, changes in the geometry have the largest effect there. Given the large bandwidth and the fixed frequency operation of the cavity tuning is probably not required. A rather straightforward way would be to move the grid axially. This gives

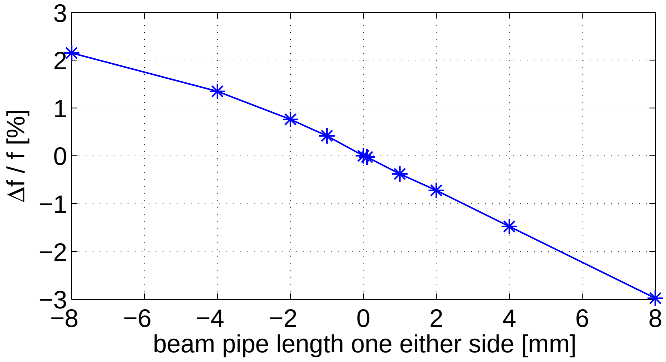

Figure 14: Change in resonant frequency as a function of the beam pipe length on either side of the cavity. Negative lengths mean that the beam pipe protrudes into the cavity.

rise to small longitudinal field inhomogeneities and the resonant frequency changes accordingly. Fig. 14 shows that a detuning in the percent range can be obtained when moving the mesh by a few mm into the beam pipe or into the cavity. Since it is complicated to have the mesh protrude into the cavity, the cavity could be built shorter and the exact position of the meshes could be adjusted by the insertion of a shim with a suitable thickness. Tuning in a limited frequency range can also be done using the external triple stub tuner, however, it is difficult to adjust the resonance frequency and the match simultaneously.

Conclusion

Various designs for a spin-flip cavity for the ASACUSA antihydrogen experiment were studied. The main challenge consists in achieving the required field homogeneity over the large beam aperture. The most promising candidate design turned out to be a resonant stripline structure. A concrete design was presented and undesired modes, coupling elements, external circuitry and the expected power consumption discussed.

Acknowledgements

I would like to thank B. Juhasz and E. Widmann for the fruitful collaboration and F. Caspers and W. Pirkl for inspiring discussion and valuable suggestions.

References

[1] Widmann, E. et al., *Measurement of the Antihydrogen Hyperfine Structure*, CERN/SPSC 2003-009 (2003)

[2] Juhasz, B., *Private communication (2008)*

[3] http://www.cst.com

[4] Sievenpiper, D. et al., *High-Impedance Electromagnetic Surfaces with a Forbidden Frequency Band*, IEEE MTT, Vol. 47, No 11 (1999)